**International Journal of Power Electronics and Drive System (IJPEDS)**
Vol. 16, No. 3, September 2025, pp. 1881∼1896
ISSN: 2088-8694, DOI: 10.11591/ijpeds.v16.i3.pp1881-1896 

# Improving electrical energy efficiency through hydroelectric power and turbine optimization at the El Oued water demineralization plant in Algeria

**Khaled Miloudi[1,2], Ali Medjghou[3,4], Ala Eddine Djokhrab[1,2], Mosbah Laouamer[1,2], Souhaib Remha[1,2], Yacine Aoun[1,2]**
[1]Department of Mechanical Engineering, Faculty of Technology, University of El Oued, El Oued, Algeria
[2]UDERZA Unit, Faculty of Technology, University of El Oued, El Oued, Algeria
[3]Department of Electronics, Institute of Science, University Center of Tipaza, Tipaza, Algeria
[4]Laboratory of Advanced Automation and Systems Analysis, Department of Electronics, Faculty of Technology, University of Batna 2, Batna, Algeria

**Article Info**

***Article history:***

Received Oct 25, 2024
Revised Apr 4, 2025
Accepted May 25, 2025

***Keywords:***

Albian aquifer
Hydroelectric power
Renewable energy
Turbine-generator group
Water demineralization plant

**ABSTRACT**

This paper presents an investigation into the energy potential of the Albian aquifer in the Algerian Sahara at the El Oued water demineralization plant, focusing on its capacity to generate electrical power due to its high-pressure and high-temperature water reserves. We designed and implemented a turbine-generator system to convert hydraulic energy into electricity, achieving an average annual energy output of 1,804,560 kWh, which translates to a financial gain of approximately 345,888,600 DZD per year from energy savings. The selection of a Francis turbine was justified based on its efficiency, which ranges from 90% to 95%, and the system design was simulated using MATLAB-Simulink, demonstrating its robustness and effectiveness in managing the electrical network parameters. Our economic analysis indicates a high return on investment, confirming the feasibility of utilizing the Albian aquifer as a strategic asset for clean and reliable energy production in the region.



***Corresponding Author:***

Khaled Miloudi
Department of Mechanical Engineering, Faculty of Technology, University of El Oued
Chott City, B.P. 789, El Oued 39000, Algeria
Email: miloudi-khaled@univ-eloued.dz, khaled.miloudi.dz@gmail.com

## 1. INTRODUCTION

In Sub-Saharan Africa, over 50% of the population lacks access to clean energy, as reported by the International Energy Agency [1]. Electricity demand is projected to increase by 4.6% due to industrial growth and population increase [2]. This region must explore alternative energy sources to improve its capacity for electricity generation. Furthermore, the environmental consequences of the heavy dependence on fossil fuels require immediate action to address these challenges and promote sustainable energy solutions [3]. Industrial operations in both developed and developing nations contribute significantly to climate change through high energy consumption and emissions of pollutants linked to global warming [4]. The 2015 Paris Conference brought together world leaders to address this issue, agreeing to limit temperature increases to 2 degrees Celsius [5]. The discussions emphasized investing in renewable energy and transitioning to low-carbon emission systems to mitigate environmental impacts. Research indicates that renewable energy can effectively replace high-carbon fuels, improving economic growth through electricity sales [6]. This collective effort aims to combat climate change and promote sustainable development. The transition from fossil fuels to renewable energy is significantly influenced by advances in renewable technologies [7]. Historically, high production costs have hindered the integration of green energy into existing networks and limited its commercial viability. However, recent reductions in equipment prices have made renewable energy more accessible globally, facilitating its adoption [8]. This shift is crucial to achieve net zero emissions and combat climate change, as outlined in the Paris Agreement [9].

According to the Energy Institute's Statistical Review of World Energy, fossil fuels accounted for 81.5% of global primary energy consumption in 2023 [10], [11]. The production of electricity from renewable energy sources is an important strategy to reduce greenhouse gas emissions, as indicated [12]-[15]. Hydroelectric power is a leading renewable energy source, contributing approximately 2.5% of the total energy resources of the world and a substantial 15.9% of global electricity generation [16], [17]. Its efficiency and reliability as an electricity source are well documented in the energy sector. The Albian aquifer, located approximately 1500 meters underground, is a vast water reserve in the Algerian Sahara [18], [19]. It serves not only as a source of freshwater, but also as a significant energy accumulator. It is considered a strategic resource because the water emerges with a pressure of 20 bar when the valve is closed and a temperature of 60 °C. Previous studies conducted by the Sahara and Sahel Observatory (OSS) have shown that the aquifer layer can provide a continuous supply of energy for at least 40 years, with each well capable of generating up to 35 kilowatts of electrical power [20].

Hydroelectric power plants are crucial in global energy production, accounting for about 20% of the world's electricity [21]. These plants harness the energy of moving water to drive turbines, which in turn power generators to produce electricity. This well-established technology offers several advantages [22], [23], such as low marginal costs and minimal greenhouse gas emissions [24]. However, the potential of aquifer water has not been fully and rationally exploited, and the actual cost per cubic meter of water from the Albian well remains unknown. The water in this aquifer is highly energy-intensive and requires a motor of approximately 75 kW for direct utilization. It is important not to underestimate the energy content of this water, especially considering the initial energy losses.

The hydraulic power available from the operational wells is substantial, and each well is capable of producing around 50 kW. In some areas, this capacity is even higher. This hydraulic power can be efficiently converted into electrical energy using turbine-generator sets. It is essential to consider that the available hydraulic energy will diminish over time due to well aging, the construction of additional productive wells, and the increasing interference of neighboring wells in regions such as El M'Ghair, Djamaa, and Touggourt. Therefore, the design and sizing of these turbine generator sets must take these factors into account.

Ayuan and Emetere [25] analyze the potential of wind energy generation in Yundum and Basse, employing the Weibull and Raleigh distributions. The findings indicate a significant potential for wind power, with varying densities, suggesting strong prospects for wind energy development at both locations. Furthermore, Ayua and Emetere [26], proposed a hybrid renewable energy power system (HREPS) for the Basse district of the Gambia, integrating wind and solar energy with battery storage. The optimal system, designed using PVsyst software, includes 20 photovoltaic modules and a 1 kW wind generator, capable of meeting an annual load of 2,555 MWh. The system shows reliable performance and substantial energy storage potential.

Furthermore, Emetere *et al.* [27] explore Pico hydroelectric systems as a viable energy solution for Nigeria, addressing the growing energy demands and environmental issues of the country. They evaluated the cost (738,000.00 ₦) and feasibility of the system, noting the abundance of water resources in southern Nigeria. The study highlights construction techniques, including the selection of water sources and turbines, concluding that Pico hydroelectric systems can significantly reduce dependence on fossil fuels and air pollution. These studies underscore the diverse renewable energy potentials in Africa and their role in reducing greenhouse gas emissions. Although Nigeria and The Gambia have explored Pico hydroelectric and hybrid renewable systems, respectively, Algeria's focus has been on harnessing the hydraulic energy of the Albian aquifer.

Our work specifically addresses the conversion of this aquifer's high-pressure and high-temperature water reserves into electrical power, a resource that has not been fully exploited in the El Oued region in the Algerian Sahara. The study focuses on:

– Design and implementation: Developing a turbine-generator system to convert the aquifer's hydraulic energy into electricity;

- Energy output and financial gains: Achieving an average annual energy output of 1,804,560 kWh, with a financial gain of 345,888,600 DZD per year due to energy savings;
- Technology selection: Justifying the use of a Francis turbine for its high efficiency (90%-95%);
- Simulation and validation: Simulating the system using MATLAB-Simulink to demonstrate its robustness and effectiveness in managing electrical network parameters; and
- Economic feasibility: Conduct an economic analysis to confirm the high return on investment and validate the feasibility of utilizing the aquifer as a strategic clean energy resource.

## 2. MATERIALS AND METHODS

### 2.1. The study area and data source description

The Albien aquifer is located largely in the Algerian Sahara and is the largest freshwater reserve in the world, see Figure 1. Covers an area of 650,000 km² [18]. Groundwater reserves include shallow aquifers, typically under 100 meters deep, which are recharged by surface water, rain, or wastewater. However, high salinity limits their agricultural use. The Albian aquifer, spanning over a million km² beneath Algeria, Tunisia, and Libya, holds approximately 31,000 billion m³ of water. In El Oued, four Albian wells supply a demineralization plant with a capacity of 30,000 m³ per day, processing water at a flow rate of 540 m³/hour and a pressure of around 5 bar. These reserves are crucial for regional water supply and management. These wells act as pumps with a well-defined operating point, see Figure 2(a).

Figure 2(b) displays the components of hydroelectric plants. The operational process of a hydroelectric power plant consists of four primary phases:

- Phase 1: Water is channeled through conduits known as forced driving, building up significant pressure;
- Phase 2: The powerful flower spins the turbines within the generator, converting kinetic energy to electrical;
- Phase 3: The generated electricity is then passed through a transformer to increase it to a high-voltage current; and
- Phase 4: The high voltage electricity is then fed into the power grid for distribution to metropolitan areas.

### 2.2. Technical importance of the Francis turbine and theoretical calculations

The search for technically secure and economically viable solutions for the exploitation of hydraulic sites has led, over the years, to a small number of types of turbines [28]. Each of these types has a preferred field of application. Without mentioning mini-hydraulics, whose selection criteria are based on other foundations, we distinguish three families of turbines for the generation of industrial hydroelectric power [29]. Table 1 provides another assessment of the differences between the main types of turbines.

Another key factor in selecting the appropriate turbine type is the specific speed. This parameter represents the rotational speed in revolutions per minute (rpm) of a turbine operating under a unit head and generating a unit of power output. Impulse turbines typically have low specific speeds, Francis turbines fall in the medium range, and propeller or Kaplan turbines exhibit high specific speeds. The specific speed of a turbine can be calculated using (1) [30], [31].

$$n_q = n \cdot \frac{Q^{1/2}}{E^{3/4}} \tag{1}$$

Where, $n = 60 \cdot \frac{f}{p}$ and $E = g \cdot H$; with: $n$ is the rotational speed of the turbine in (rpm); $Q$ is the flow in (m³/s); $f$ is the frequency of the electric system in (Hz); $p$ is the number of pairs of poles of the trubine generator; E is the specific hydraulic energy of the machine in (J/kg); $g$ is the gravitational constant in (m/s²); $H$ is the net head in (m).

The range of head is a critical factor in selecting the appropriate turbine for a specific site, as it directly influences the turbine's performance and efficiency. Table 2 represents the range of operating heads for different types of turbine used in the generation of hydroelectric power. Table 2 provides a criterion for estimating a suitable turbine for a hydroelectric project based on the net head, which is the height of standing water available for power production.

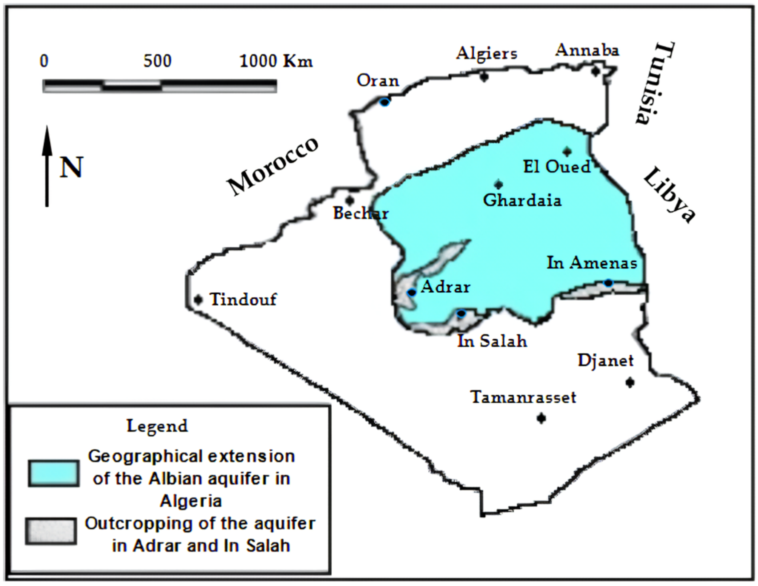


Figure 1. Location of the aquifer's existence in Algeria

(a)

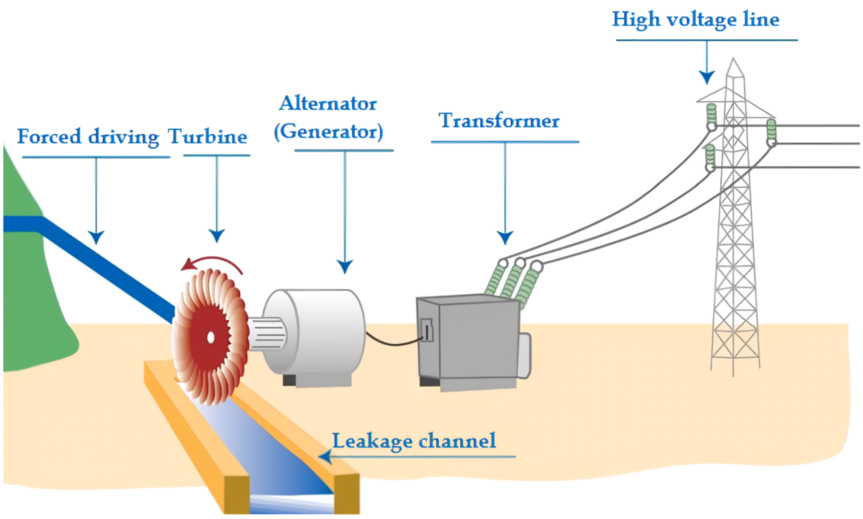


(b)

Figure 2. Components and operational phases of hydroelectric power plants: (a) Albian drilling in El Oued (Touggourt road) and (b) working principle of hydroelectric power plant

Table 1. Comparison for the three main types of turbines [29]

| Parameter | Francis | Pelton | Kaplan |
|---|---|---|---|
| Specific speed (rpm) | 30 to 400 | 3 to 36 | 300 to 1000 |
| Drop height (m) | 15 to 300 | 100 to 1000 | 2 to 30 |
| Power up to (MW) | 15 | 15 | 15 |
| Efficiency (%) | 94 | 93 | 94 |

Table 2. Range of head [32]

| Turbine type | Typical range of heads ($H$ = head in $m$) |
|---|---|
| Kaplan and Propeller | $2 < H < 40$ |
| Francis | $25 < H <350$ |
| Pelton | $50 < H < 1300$ |

### 2.3. Choice of a supplier

Following our online research and review of potential turbine suppliers, we engaged with a Chinese supplier. After sharing our requirements, they suggested that a Francis turbine with 200 kW type HLA550-WJ-45 capacity would be the most suitable for our needs, particularly for driving the cooling tower machines which have a combined power of 150 kW. The technical specifications for both the generator and the turbine, including accessories, along with the purchase price in US dollars, are listed in Tables 3 and 4.

### 2.4. The current generator

Once in motion, the turbine drives the current generator, which transforms the mechanical energy available on the shaft into electrical energy. The frequency of the current generator is a multiple of the number of revolutions of the drive shaft. The generator is separated from the turbine by a special shield that protects it from any contact with water. The choice of generator essentially depends on the use of the energy produced.

### 2.5. Mechanical power

The mechanical power generated by the turbine can be calculated using (2). Where $P_{mec}$ is the mechanical power of the turbine shaft (W), $W$: Work done (J), $t$ is the time duration (s), $F$ is the force applied on the turbine blades (N), $l$ is the distance moved by the force (m), $v$ is the velocity of the turbine blades (m/s), $w$ is the angular velocity of the turbine shaft (rad/s), $R$ is the radius of the turbine (m), $C$ is the torque exerted on the turbine shaft (N·m).

$$P_{mec} = \frac{W}{t} = \frac{F \cdot l}{t} = F \cdot v = w \cdot F \cdot R = w \cdot C \quad (2)$$

### 2.6. Electric power

Electrical power is the power directly available at the generator output. It is obtained from the voltage, current, and power factor provided by the manufacturer, as well as the exploitable potential (hydraulic power) and the efficiencies of the turbine and generator.

$$P_{elec} = \eta_t.\eta_g.Q.\rho.E \quad (3)$$

Where $P_{elec}$ is the electrical power, $\eta_t$ is the turbine efficiency at flow $Q$, $\eta_g$ is the generator efficiency, $\rho$ is the density of water (kg/m³).

The actual power output of a small hydroelectric plant for a given flow rate $Q$ is obtained from (4).

$$P_T = \int P_{elec} \cdot dt \Rightarrow P_T = \eta_t.\eta_g.Q.\rho.g.H \int dV \quad (4)$$

Where $P_T$ is the total electrical energy generated (J), $g$ is the acceleration due to gravity (m/s²), $H$ is the net head or height difference of water (m), $dV$ is the differential volume of water (m³).

Table 3. 200 kW hydro turbine generator quotation sheet

| Name | Unit price (USD) | Quantity | Picture |
|---|---|---|---|
| Hydro turbine HLA550-WJ-45 | 1 set | 21,700 |  |
| Generator SFW200-6/650 | 11,590 | 1 set |  |
| Governor YWT-300 (Microcomputer) | 7,930 | 1 set |  |
| Electric gate valve Z945T-10DN350 | 2,170 | 1 set |  |
| Generator integrated protection screen PKF-W-200/400 | 5,070 | 2 units |  |

Table 4. Configuration list of hydroelectric power plant

| Parameters | Description | Value |
|---|---|---|
| Basic | Design head $H_r$ (m) | 50 |
| | Maximum head $H_{max}$ (m) | – |
| | Minimum head $H_{min}$ (m) | – |
| | Design discharge $Q$ (m³/s) | 0.5 |
| | Installed capacity $N$ (kW) | 200 |
| | Altitude $\nabla$ (m) | – |
| Turbine | Turbine type | HLA550-WJ-45 |
| | Layout pattern | Horizontal |
| | Runner diameter $D_l$ (cm) | 45 |
| | Unit speed $n_{11}$ (r/min) | 63.6 |
| | Unit discharge $Q_{11}$ (L/s) | 349 |
| | Model efficiency (design point) $\eta_m$ (%) | 92.7 |
| | Prototype efficiency $\eta_t$ (%) | 88 |
| | Max. model efficiency $\eta_t$ (%) | 92.7 |
| | Rated speed $n$ (r/min) | 1000 |
| | Rated output $P$ (kW) | 215.8 |
| | Max. axial hydraulic thrust $P_Z$ (T) | 1 |
| | Cavitation coefficient $\sigma$ | 0.055 |
| | Runaway speed $n_R$ (r/min) | 1752 |
| | Weight of runner (t) | 2 |
| | Turbine weight (t) | 0.02 |
| | Max. hoisting piece (Turbine) (t) | 3 |
| Generator | generator type | SFW200-6/650 |
| | Layout pattern | Horizontal |
| | Rated power $P$ (kW) | 200 |
| | Rated voltage $V$ (V) | 400 |
| | Rated current $I$ (A) | 360.9 |
| | Power factor cos $\phi$ | 0.8 (lagging) |
| | Excitation voltage (V) | 40 |
| | Excitation current (A) | 116 |
| | Generator efficiency $\eta_g$ (%) | 93 |
| | Generator speed $n$ (r/min) | 1000 |
| | Number of phases | 3 |
| | Frequency $f$ (Hz) | 50 |
| | Insulation class | F/F |
| | Excitation mode | Brushless exciter |
| | Generator weight (t) | 3 |
| | Max. hoisting piece (generator) (t) | 3 |

### 2.7. Calculation of hydroelectric power of a turbine

To calculate the power output of a hydroelectric turbine, the basic formula is given by (5).

$$P_{hyd} = \rho.Q.g.H.\eta \tag{5}$$

Where: $\rho$ : density of water (kg/m³), $Q$ : water flow rate in the pipeline (m³/s), $g$ : Newton's gravitational constant (m/s²), $H$ : Waterfall height (m), $\eta$ : efficiency ratio (typically between 0.7 and 0.9).

### 2.8. Efficiency

The Francis turbine is highly efficient, achieving performance levels of 90% to 95%. Its exceptional efficiency is due to the blade design that utilizes both reaction and impulse forces from flowing water. The quality of the turbine is measured by its efficiency $\eta_t$, which indicates the ratio between two powers.

$$\eta_t = \frac{P_{mec}}{P_{hyd}} \tag{6}$$

Where $P_{hyd}$ is hydraulic power.

The efficiency of the generator also takes the same form, as (7).

$$\eta_g = \frac{P_{elec}}{P_{mec}} \tag{7}$$

However, it is common to consider an overall efficiency of the turbine-generator set, which is as (8).

$$\eta_T = \frac{P_{elec}}{P_{hyd}} = \frac{P_{elec}}{P_{mec}}\frac{P_{mec}}{P_{hyd}} = \eta_t.\eta_g \tag{8}$$

This overall efficiency varies between 0.7 and 0.9, depending on the type of turbine and generator used. The electrical energy produced over one year is the main factor in determining the profitability of the work.

## 2.9. Calculation of hydroelectric energy production of a turbine

We will apply the parameters we have to calculate the exploitable power. Water energy potential: if we take the data we have for the 04 wells: flow rate: 0.5 $m^3/s$, pipeline diameter: 630 cm, pipeline section: 28.2743 $m^2$, gravitational constant: 9.81 $m/s^2$, waterfall height: 50 m, and density: 1000 $kg/m^3$ (typically 1000 $kg/m^3$ for water).

After applying as (8), we obtain the maximum power before losses: 245 kW. Efficiency losses and actual electrical energy available at the turbine outlet: after obtaining the electrical and mechanical efficiencies of the plant from a manufacturer, which are: turbine efficiency: 92%, head loss coefficient: 95%;, other losses: 98%, and overall efficiency: 81%. We have found that the useful electrical power is: 206 kW.

## 2.10. Effects of turbine integration on the functioning of the water demineralization plant

The water emerges from the well under pressure ranging from 10 to 30 bars and at a temperature between 40 °C and 80 °C. Then it travels through transfer pipes to the top of the cooling tower, as shown in Figure 3(a). Despite its abundance, water is not suitable for immediate human consumption because of its high temperature. The water then passes through openings in the cooler and is cooled to 25 °C at the top of the cooling tower by forced ventilation, which promotes heat transfer through evaporation. This cooling process involves dispersing the water into fine droplets on metal slats. As atmospheric air comes into contact with water, it absorbs heat and changes from ambient humidity levels to near saturation by evaporating a portion of the water intended for cooling, as depicted in Figure 3(b). Since the cooling process involves forced ventilation, the extraction of hot and humid air is carried out by means of an extractor fan with a diameter of 5 meters Figure 3(c), which requires a motor with a power of 75 kW operating at 380 V Figure 3(d). Table 5 provides detailed characteristics of the electric motor used in the hydroelectric power system described in the study.

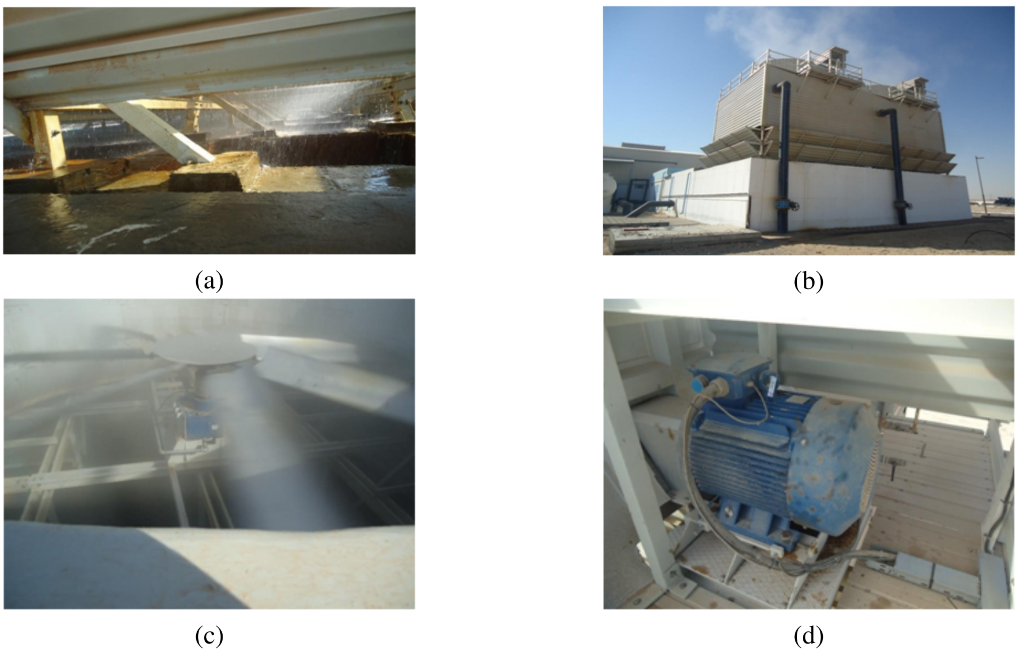

Figure 3. Enhancing cooling efficiency and water quality: (a) water outlet at the cooler, (b) pipeline for conveying well water, (c) cooler hot air extractor, and (d) motor used at cooling tower top

Table 5. Motor characteristics

| Type | Value | Picture |
|---|---|---|
| Motor size/service factor | 280 M4 / 1.1 |  |
| Number of poles | 4 | |
| Instantaneous unit power | 75 kW | |
| Instantaneous module power | 75 kW | |
| Total instantaneous power | 150 kW | |
| Absorbed unit power | 67.5 kW | |
| Absorbed module power | 67.5 kW | |
| Total absorbed power | 135 kW | 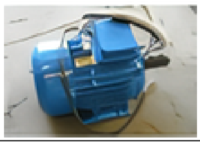 |
| Speed | 1440 Rpm | |
| Voltage/frequency | 400/50 Volt/Hz | |
| Insulation class | IP55 module | |
| Protection type | F/B module | |

Note: Electric motor type: totally enclosed fan cooled (TEFC) asynchronous 3-phase motor with special high-quality bearings (SKF type 2RSC3) lubricated for life and are totally watertight

### 2.11. Rotational speed of the turbine-generator group

The rotation speeds of synchronous generators vary depending on the number of poles they have: 1 pair of poles (n = 3000 rpm), 2 pairs of poles (n = 1500 rpm), 3 pairs of poles (n = 1000 rpm), 4 pairs of poles (n = 750 rpm), 5 pairs of poles (n = 600 rpm), and 6 pairs of poles (n = 500 rpm). In practice, the maximum speed is limited to 1500 rpm (2 pole pairs) to account for overspeed during run-up. Exceeding this speed can cause significant mechanical stress. As a result, generators with a single pole pair are rarely installed (run-up speed of 6000 rpm). Below 6000 rpm (6 pole pairs or more), the size of the generator, and thus its cost relative to the installed power, increases, while efficiency decreases due to increased losses, particularly magnetic losses. When the turbine rotation speed is below 600 rpm, it typically drives a low-pole generator (1000 or 1500 rpm) through a belt drive or a gear multiplier, for example.

### 2.12. Consequences of turbine integration

Integrating turbines into the system involves installing turbine-generator units on the cooling tower's roof, which requires modifications to the existing pipeline to maintain adequate pressure upstream. A shut-off valve and a bypass valve are essential at the turbine inlet. This integration capitalizes on the synergy between hydraulics and mechanics, allowing the utilization of previously wasted energy. Before integration, the water exited at high pressure, passed through the pipeline, and ended up at atmospheric pressure, resulting in energy loss. After turbine installation, even minimal energy is harnessed, making it cost-effective over time. The hydroelectric plant can recover all the energy needed to operate the two 75 kW cooling tower motors, with the selected turbine rated at 200 kW.

### 2.13. Economic considerations

Hydroelectric energy production and financial gain: We can estimate the gain that can be achieved after one year of operation of the power plant as shown: The average annual energy production of the hydroelectric turbine is estimated at 1,804,560 kWh, which translates to a total financial gain of 345,888,600 DZD/year based on an energy cost of 265 DZD per kW saved. Furthermore, we have included a breakdown of the initial investment required for the power plant, which is approximately 7,200,000 DZD. This analysis highlights the potential for significant long-term savings, as the return on investment is projected to be achieved within a few years of operation, considering the high efficiency of the selected Francis turbine, which operates at an efficiency rate of 92%. Furthermore, we discuss the implications of reduced operational costs due to the integration of the turbine-generator system, which allows the recovery of energy that would otherwise be wasted, thereby enhancing the overall economic viability of the project. By incorporating these detailed financial analyses, we aim to provide a more robust economic framework that supports the feasibility and sustainability of the proposed system.

### 2.14. Simulation setup

The generator model in our study is a synchronous generator with salient poles, featuring three stator windings, one rotor winding, and two damper windings. The simulation will utilize specific mathematical equations [33]-[35] that describe the relationship between the currents, voltages, and fluxes in each winding.

Following the application of the Park transformation to these equations, the model is represented in unit form (pu), encompassing electrical voltage and current equations, as well as mechanical equations.

The quantities used at the input of a power system stabilizer (PSS) are generated by the rotation speed of the shaft, the frequency, and the power [36], [37]. The PSS is designed to dampen power oscillations, particularly in weak signal conditions, thereby enhancing stability. It was in conjunction with the automatic voltage regulator (AVR) [38] by providing an additional input to the excitation system. For the mathematical modeling of the generator to study its dynamic behavior, the following simplifying hypotheses will be considered:

- Assumption 1: We assume that the magnetic circuit is unsaturated and perfectly laminated, allowing us to focus on the currents flowing through the windings (inductor, induced, and dampers).
- Assumption 2: We will represent the complete set of dampers with two simplified windings: one aligned with the direct axis (d) and the other with the quadrature axis (q).

The turbines are powered by the water that comes from the well. Their speed regulation system is ensured by regulating valves, which play an essential role not only in regulating the output speed and power of the turbine but also in adjusting the extraction pressure.

The main goal is to control the output values of the electrical network parameters (voltage and current). The complete hydraulic turbine–synchronous generator model represents a dynamically modeled hydroelectric power plant in Simulink/MATLAB (as shown in Figure 4). It enables simulation of the overall system and analysis of interactions between the various control subsystems. In Figure 4, the hydraulic turbine converts the energy of water (flow rate and pressure) into mechanical energy, taking into account efficiency and losses. Provides mechanical torque and power to the generator. The synchronous generator, modeled in the Park transformation, transforms this mechanical energy into electrical energy in the form of three-phase voltage and active/reactive power. The ST1 excitation system uses a PID controller to maintain a stable output voltage, with built-in protection limiters. It receives the reference voltage and a signal from the power system stabilizer (PSS), which acts on the excitation to improve stability by damping oscillations caused by network disturbances. The governor regulates the water flow based on the difference between the actual and reference speed, ensuring mechanical stability. The model displays various electrical variables (voltage, current, flux, and power) and mechanical variables (torque and speed).

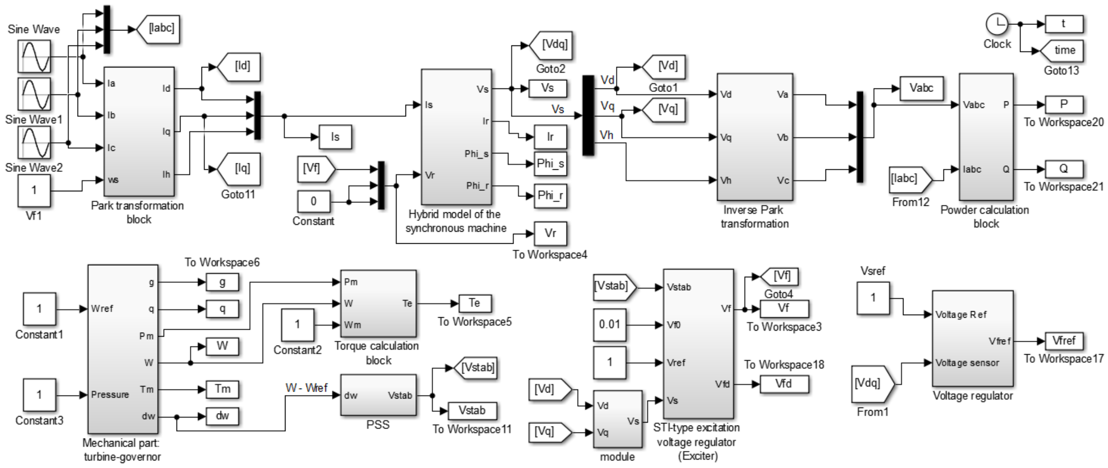

Figure 4. Block diagram of the overall control system

## 2.15. Voltage regulation in the overall system

The hybrid model of the synchronous machine is combined with the ST1 static excitation system, as standardized by IEEE and detailed in [18], [39]. Tables 6-8 provide the main parameters of the turbine-generator. The simulation results follow the implementation in MATLAB Simulink.

Table 6. Parameters of synchronous generator

| Parameter | | Symbol | Value |
|---|---|---|---|
| Main parameter | Apparent power | S | 200 kW |
| | Nominal stator voltage | V | 400 V |
| | Maximum stator current | I | 360 A |
| | Frequency | F | 50 Hz |
| | Rotation speed | N | 1000 rpm |
| | Number of pole pairs | P | 3 |
| Resistance in $pu$ unit | Stator resistance | $R_s$ | 0.026 |
| | Leakage resistance | $R_r$ | - |
| Reactance in $pu$ units | d and q axes synchronous | $X_d$ | 0.669 |
| | | $X_q$ | 0.3417 |
| | d and q axes transient | $x'_d$ | 0.18 |
| | | $x'_q$ | 0.36 |
| | d and q axes sub-transient | $x''_d$ | 0.13 |
| | | $x''_q$ | 0.09 |
| | Stator leak | $x_f$ | 0.09 |
| | Kany reactance K$enty$ | $x_{kf1}$ | -0.0081 |

Table 7. Parameters of static excitation system ST1

| Parameter | Value | | | |
|---|---|---|---|---|
| Voltages limitation | $V_{Amax} = 400$ | $V_{Amin} = -400$ | $V_{Rmax} = 40$ | $V_{Rmin} = -40$ |
| Voltages limitation | $V_{Amax} = 400$ | $V_{Amin} = -400$ | $V_{Rmax} = 40$ | $V_{Rmin} = -40$ |
| Currents limitation | $V_{Imax} = 116$ | $V_{Imin} = -116$ | $-$ | $-$ |
| Rectification | $K_c = 0.04$ | $K_{LR} = 1$ | $-$ | $-$ |
| Automatic voltage | $K_A = 1.62$ | $K_f = 0.0503$ | $K_E = 1$ | $T_b = 1$ |
| Regulator (AVR) | $T_A = 0.0087$ | $T_f = 0.3774$ | $T_E = 0$ | $T_c = 1$ |
| Classic regulator PID | $K_P = 1.13\ .10^{-4}$ | $K_I = 6.3496$ | $K_D = 0.0082$ | $-$ |
| Parameter of stabilizing transformer in $(pu)$ | $R_t = 0.0159$ | $L_I = 0.006$ | $M = 0.8\ .10^{-3}$ | $-$ |

Table 8. Ideal parameters of hydraulic turbine

| Parameter | Symbol | Value |
|---|---|---|
| Nominal power | $P_m$ | 215 MW |
| Winnowing | $g_{max}$ | Nominal opening: 5 pu |
| | $g_0$ | Opening when empty: 0.02 pu |
| Nominal water flow | Q | 0.5 m³/s |

## 3. RESULTS AND DISCUSSIONS

Figure 5 illustrates the regulation of voltages in the overall system, which is crucial to maintaining the stability and efficiency of the electrical network. This figure is part of the discussion on how the hybrid model of the synchronous machine, combined with the static excitation system, operates to stabilize the generator's output voltage. Proper voltage regulation is essential to ensure that the system can respond effectively to fluctuations and maintain consistent performance.

### 3.1. Effectiveness tests of the system

We will conduct two simulation experiments. The first will involve inducing a change in pressure. The second will involve disconnecting the PSS to observe the system's reaction, its speed, and its accuracy compared to the previous results.

Effectiveness test by varying pressure: We will create a scenario to introduce a disturbance and observe the system response. This will involve adjusting the pressure value to 1.5 $pu$, which deviates from the standard pressure value of 1 $pu$. Figure 6 illustrates the effectiveness test carried out by varying the pressure within the system. This test was designed to observe the response of the system to a disturbance introduced by adjusting the pressure value to 1.5 pu, deviating from the standard pressure value of 1 pu. The results showed favorable response speeds and a decrease in amplitude, indicating that the power system stabilizer (PSS) effectively mitigated the effects of the pressure change without disrupting other components of the system.

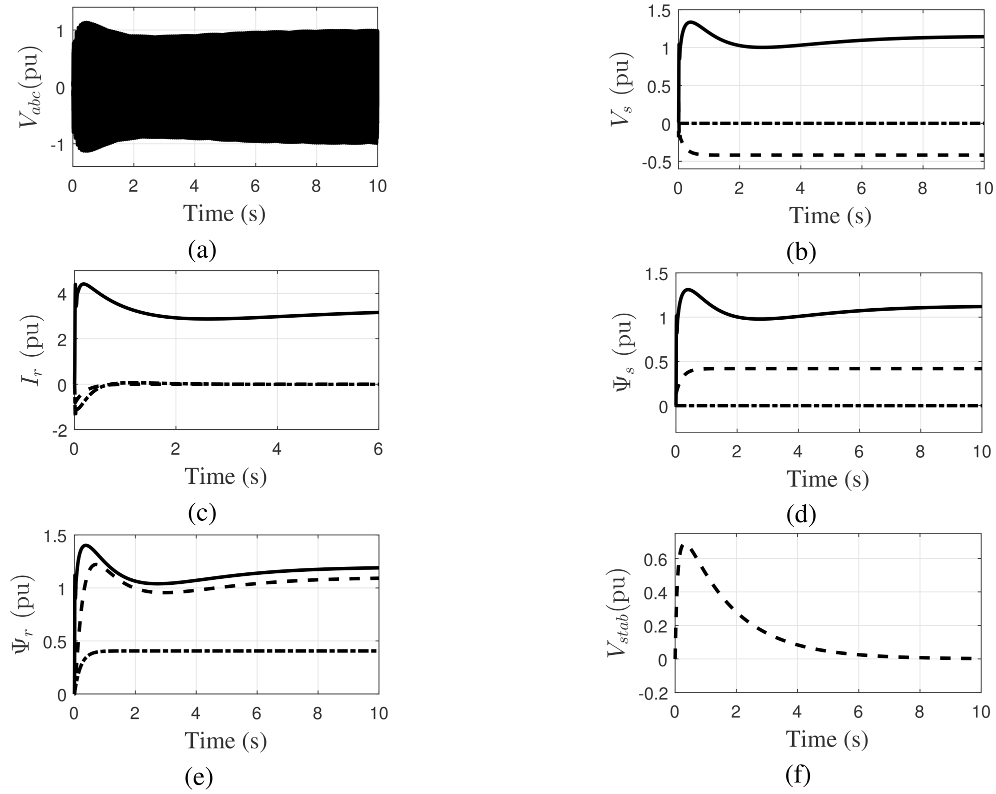


Figure 5. Regulation of voltages in the overall system: (a) generator output voltage $V_{abc}$, (b) stator voltage vector $V_s$, (c) rotor current vector $I_r$, (d) stator flow hybrid model $\Psi_s$, (e) rotor flow hybrid model $\Psi_s$, and (f) stabilization voltage $V_{stab}$

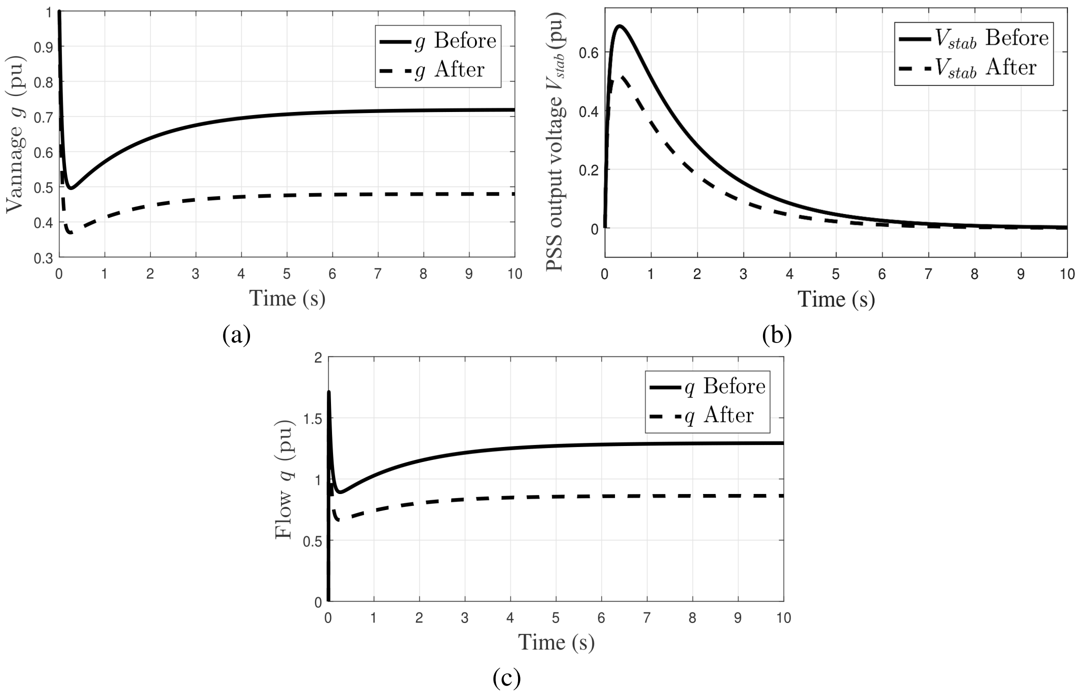


Figure 6. Effectiveness test through pressure variation: (a) variation in the vannage $g$, (b) variation in the PSS output voltage $V_{stab}$, and (c) flow variation $q$

Effectiveness test by isolating the PSS: We create a scenario to introduce a disturbance and observe the system response. This involves removing the PSS and comparing the simulation results before neglecting it, as in Figure 7. In this test, Figure 7, the system's response was analyzed with and without the power system stabilizer (PSS) during transient disturbances, specifically between 0 and 0.5 seconds. When the PSS was removed, the response was slower and smoother, with no overshoots, highlighting the stabilizer's crucial role in maintaining generator voltage stability. When the PSS was active, the response was faster and exhibited some overshoots, but the system stabilized quickly after that. The study emphasizes the importance of regulators in electrical networks, showing their ability to restore generator stability after transient errors. The simulation results clearly demonstrate the PSS's effectiveness in improving system performance during disturbances.

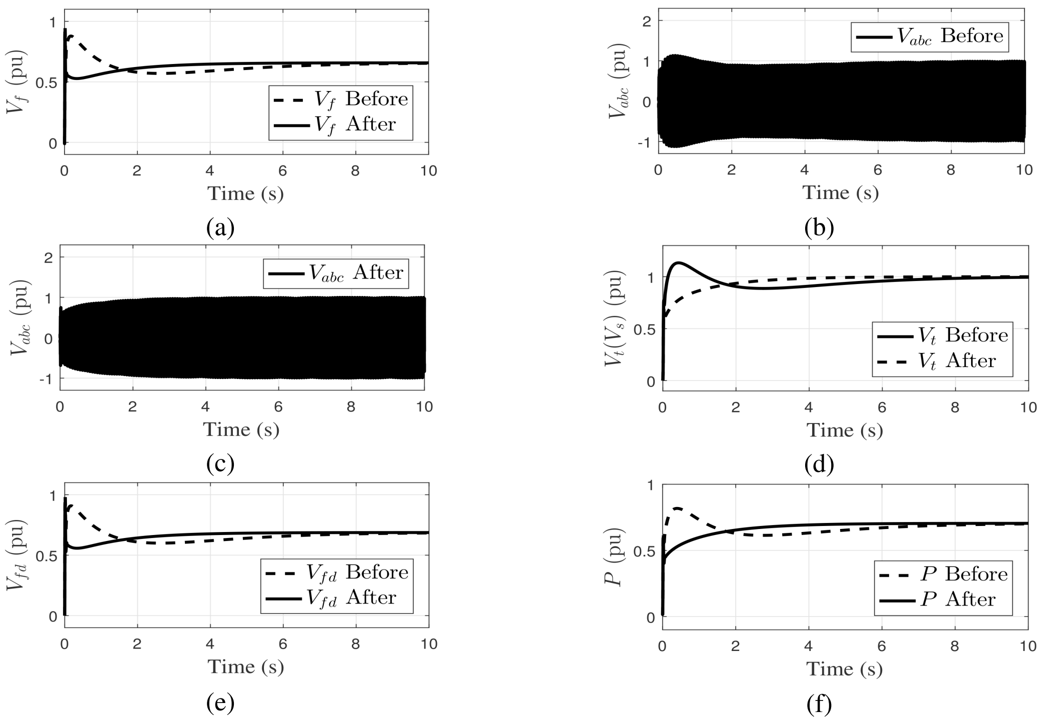


Figure 7. Efficiency test through isolation of the PSS: (a) load voltage $V_F$, (b) voltage $V_{abc}$, (c) voltage $V_{abc}$, (d) terminal voltage $V_t(V_s)$, (e) AVR output voltage $V_{fd}$, and (f) active power $P$

## 4. CONCLUSION

The study conducted at the El Oued water demineralization plant successfully demonstrated the potential of the Albian aquifer as a reliable and sustainable energy source. The impact and limitations of our work are outlined as follows: i) Advancement in renewable energy utilization: This study demonstrates the effective conversion of the Albian aquifer's hydraulic energy into electrical power, showcasing a novel approach to harnessing renewable energy in the Algerian Sahara, which has not been fully exploited previously; ii) Economic benefits: The implementation of the hydroelectric system results in an average annual energy output of 1,804,560 kWh, translating to a financial gain of approximately 345,888,600 DZD per year from energy savings. This highlights the economic viability of renewable energy solutions in the region; iii) High efficiency of technology: The selection of a Francis turbine, which operates at an efficiency rate of 90% to 95%, underscores the technological advancements in turbine design that enhance energy conversion efficiency; and iv) Environmental impact: By reducing reliance on fossil fuels and promoting the use of renewable energy, this research contributes to mitigating climate change and supports global efforts to transition to low-carbon energy systems.

## FUNDING INFORMATION

The authors declare no funding involved.

## AUTHOR CONTRIBUTIONS STATEMENT

This journal uses the Contributor Roles Taxonomy (CRediT) to recognize individual author contributions, reduce authorship disputes, and facilitate collaboration.

| Name of Author | C | M | So | Va | Fo | I | R | D | O | E | Vi | Su | P | Fu |
|---|---|---|---|---|---|---|---|---|---|---|---|---|---|---|
| Khaled Miloudi | ✓ | ✓ | ✓ | ✓ | ✓ | ✓ | ✓ | ✓ | ✓ | ✓ | ✓ | | ✓ | |
| Ali Medjghou | ✓ | ✓ | ✓ | ✓ | ✓ | ✓ | ✓ | ✓ | ✓ | ✓ | ✓ | | | |
| Ala Eddine Djokhrab | ✓ | | ✓ | | ✓ | ✓ | ✓ | | | ✓ | ✓ | | | |
| Mosbah Laouamer | ✓ | | ✓ | | ✓ | ✓ | ✓ | | | ✓ | ✓ | | | |
| Souhaib Remha | ✓ | | ✓ | | ✓ | ✓ | ✓ | | | ✓ | ✓ | | | |
| Yacine Aoun | ✓ | ✓ | ✓ | ✓ | ✓ | ✓ | ✓ | | | ✓ | ✓ | ✓ | ✓ | |

C : **C**onceptualization
M : **M**ethodology
So : **So**ftware
Va : **Va**lidation
Fo : **Fo**rmal Analysis
I : **I**nvestigation
R : **R**esources
D : **D**ata Curation
O : Writing - **O**riginal Draft
E : Writing - Review & **E**diting
Vi : **Vi**sualization
Su : **Su**pervision
P : **P**roject Administration
Fu : **Fu**nding Acquisition

## CONFLICT OF INTEREST STATEMENT

The authors declare no conflict of interest.

## DATA AVAILABILITY

No data was used for the research described in the paper.

## REFERENCES

[1] IEA, IRENA, UNSD, World Bank, and WHO, "Tracking SDG 7: The energy progress report," Washington DC, 2022. [Online]. Available: https://www.irena.org/-/media/Files/IRENA/Agency/Publication/2022/Jun/SDG7_Tracking_Progress_2022.pdf.

[2] IEA, "Assessing the effects of economic recoveries on global energy demand and CO2 emissions in 2021," 2021. [Online]. Available: https://iea.blob.core.windows.net/assets/d0031107-401d-4a2f-a48b-9eed19457335/GlobalEnergyReview2021.pdf.

[3] O. Ellabban, H. Abu-Rub, and F. Blaabjerg, "Renewable energy resources: Current status, future prospects and their enabling technology," *Renewable and Sustainable Energy Reviews*, vol. 39, pp. 748–764, Nov. 2014, doi: 10.1016/j.rser.2014.07.113.

[4] A. A. Tyovenda, T. J. Ayua, and T. Sombo, "Modeling of gaseous pollutants (CO and NO2) emission from an industrial stack in Kano city, northwestern Nigeria," *Atmospheric Environment*, vol. 253, p. 118356, May 2021, doi: 10.1016/j.atmosenv.2021.118356.

[5] D. Icaza and D. Borge-Diez, "Technical and economic design of a novel hybrid system photovoltaic/wind/hydrokinetic to supply a group of sustainable buildings in the shape of airplanes," *Heliyon*, vol. 9, no. 3, 2023, doi: 10.1016/j.heliyon.2023.e14137.

[6] R. Alvarado *et al.*, "Do economic development and human capital decrease non-renewable energy consumption? Evidence for OECD countries," *Energy*, vol. 215, p. 119147, Jan. 2021, doi: 10.1016/j.energy.2020.119147.

[7] O. R. Katoch, R. Sharma, S. Parihar, and A. Nawaz, "Energy poverty and its impacts on health and education: a systematic review," *International Journal of Energy Sector Management*, vol. 18, no. 2, pp. 411–431, Feb. 2024, doi: 10.1108/IJESM-10-2022-0007.

[8] A. Shaqour, H. Farzaneh, Y. Yoshida, and T. Hinokuma, "Power control and simulation of a building integrated stand-alone hybrid PV-wind-battery system in Kasuga City, Japan," *Energy Reports*, vol. 6, pp. 1528–1544, Nov. 2020, doi: 10.1016/j.egyr.2020.06.003.

[9] S. Jacobsson and A. Johnson, "The diffusion of renewable energy technology: an analytical framework and key issues for research," Energy Policy, vol. 28, no. 9, pp. 625–640, Jul. 2000, doi: 10.1016/S0301-4215(00)00041-0.

[10] F. Manzano-Agugliaro, F. G. Montoya, A. Sabio-Ortega, and A. García-Cruz, "Review of bioclimatic architecture strategies for achieving thermal comfort," *Renewable and Sustainable Energy Reviews*, vol. 49, pp. 736–755, 2015, doi: 10.1016/j.rser.2015.04.095.

[11] KPMG and KEARNEY, "73rd statistical review of world energy," *Energy Institute*, London, United Kingdom, 2024.

[12] V. Yildiz and J. A. Vrugt, "A toolbox for the optimal design of run-of-river hydropower plants," *Environmental Modelling & Software*, vol. 111, pp. 134–152, Jan. 2019, doi: 10.1016/j.envsoft.2018.08.018.

[13] S. Karmich, E. Ziani, J. Bouchnaif, and M. El-Malki, “Impact of integration of renewable energies and energy efficiency on the reliability of the national electricity grid,” *International Journal of Power Electronics and Drive Systems (IJPEDS)*, vol. 14, no. 4, pp. 2433-2446, Dec. 2023, doi: 10.11591/ijpeds.v14.i4.pp2433-2446.

[14] I. M. A. Nugraha and I. G. M. N. Desnanjaya, “Optimization of renewable energy-based electrical systems on tourist ships in Labuan Bajo,” *International Journal of Power Electronics and Drive Systems (IJPEDS)*, vol. 16, no. 2, pp. 1306-1313, Jun. 2025, doi: 10.11591/ijpeds.v16.i2.pp1306-1313.

[15] O. R. Katoch, “Exploring the relationship between expenditure on power and state finances: an empirical study in Jammu and Kashmir, India,” *Environment, Development and Sustainability*, vol. 26, no. 10, pp. 2023, doi: 10.1007/s10668-023-03734-8.

[16] O. Bozorg Haddad, M. Moradi-Jalal, and M. A. Mariño, “Design–operation optimisation of run-of-river power plants,” *Proceedings of the Institution of Civil Engineers - Water Management*, vol. 164, no. 9, pp. 463–75, 2011, doi: 10.1680/wama.2011.164.9.463.

[17] T. R. Jadoon, M. K. Ali, S. Hussain, A. Wasim, and M. Jahanzaib, “Sustaining power production in hydropower stations of developing countries,” *Sustainable Energy Technologies and Assessments*, vol. 37, 2020, doi: 10.1016/j.seta.2020.100637.

[18] S. Ouali, “Geothermal study of southern Algeria (in French: *Etude géothermique du sud de l’Algerie*),” M’hamed Bougara University, 2005.

[19] S. Ouali and A. Bouguern, “Characterization study of the Albian reservoir of southern Algeria,” *Journal of Renewable Energies*, vol. 19, no. 4, pp. 525–531, Oct. 2023, doi: 10.54966/jreen.v19i4.591.

[20] OSS, “Northern Sahara Aquifer System: Hydrogeology, Volume II (in French: *Système Aquifère du Sahara Septentrional: Hydrogeologie, volume II*),” Algeria, Libya, Tunisia, 2003. [Online]. Available: https://www.oss-online.org/fr/releases/OSS-SASS_HYDROGEOLOGIE.

[21] MBT Electrical Equipment JSC, “Structure and working principle of hydroelectric power plant,” Vietnam Transformer. Accessed: Jun. 24, 2024. [Online]. Available: https://vietnamtransformer.com/our-news/structure-and-working-principle-of-hydroelectric-power-plant.

[22] J. C. Casila, M. Duka, R. De Los Reyes, and J. C. Ureta, “Potential of the Molawin creek for micro hydro power generation: An assessment,” *Sustainable Energy Technologies and Assessments*, vol. 32, pp. 111–120, Apr. 2019, doi: 10.1016/j.seta.2019.02.005.

[23] D. Tsuanyo, B. Amougou, A. Aziz, B. Nka Nnomo, D. Fioriti, and J. Kenfack, “Design models for small run-of-river hydropower plants: a review,” *Sustainable Energy Research*, vol. 10, no. 1, p. 3, Feb. 2023, doi: 10.1186/s40807-023-00072-1.

[24] B. Stoll, J. Andrade, S. Cohen, G. Brinkman, and C. Brancucci Martinez-Anido, “Hydropower modeling challenges,” Golden, CO (United States), Apr. 2017. doi: 10.2172/1353003.

[25] T. J. Ayua and M. E. Emetere, “Technical analysis of wind energy potentials using a modified Weibull and Raleigh distribution model parameters approach in the Gambia,” *Heliyon*, vol. 9, no. 9, p. e20315, Sep. 2023, doi: 10.1016/j.heliyon.2023.e20315.

[26] T. J. Ayua and M. E. Emetere, “Technical and economic simulation of a hybrid renewable energy power system design for industrial application,” *Scientific Reports*, vol. 14, no. 1, p. 28739, Nov. 2024, doi: 10.1038/s41598-024-77946-x.

[27] E. M. E, A. T. J, and A. S. A, “The prospect of Pico hydroelectric system construction for domestic application in Nigeria-a review,” in *2024 International Conference on Science, Engineering and Business for Driving Sustainable Development Goals (SEB4SDG)*, IEEE, Apr. 2024, pp. 1–5. doi: 10.1109/SEB4SDG60871.2024.10630385.

[28] J. Raabe, “Great names and the development of hydraulic machinery,” *Hydraulics and Hydraulic Research*, pp. 251–266, 1987.

[29] J.-M. Chapallaz *et al.*, *Turbines hydrauliques - Training days for engineers* (in French: *Turbines hydrauliques - Journées de formation pour ingénieurs*). 1995.

[30] H. Ramos, “Guidelines for design of small hydropower plants,” Belfast, 2000.

[31] Energy Community Platform, “Guide on how to develop a small hydropower plant,” European Small Hydropower Association—ESHA. [Online]. Available: https://energycommunityplatform.eu/wp-content/uploads/2022/06/Merged-Guide-Develop-a-Small-Hydropower-Plant.pdf.

[32] M. Taih and R. Azeez, “Hydro power,” in *Energy Conservation*, InTech, 2012. doi: 10.5772/52269.

[33] P. S. Kundur, “Power system stability,” in *Power System Stability and Control*, 3rd ed., CRC Press, 2012.

[34] C.-H. Cheng and Y.-Y. Hsu, “Damping of generator oscillations using an adaptive static VAR compensator,” *IEEE Transactions on Power Systems*, vol. 7, no. 2, pp. 718–725, May 1992, doi: 10.1109/59.141778.

[35] K. Ouramdane, “Modeling and optimization of the excitation system of the turbine-generator group of the Hydro-Québec analog simulator (in French: *Modélisation et optimisation du système d’excitation du groupe turbine-alternateur du simulatuer analogique d’Hydro-Québec*),” University of Quebec in Abitibi-Témiscamingue, 2015.

[36] W. Shao and Z. Xu, “Excitation system parameter setting for power system planning,” in *IEEE Power Engineering Society Summer Meeting*, IEEE, 2002, pp. 541–546. doi: 10.1109/PESS.2002.1043295.

[37] J. Machowski, J. W. Bialek, S. Robak, and J. R. Bumby, “Excitation control system for use with synchronous generators,” *IEE Proceedings - Generation, Transmission and Distribution*, vol. 145, no. 5, p. 537, 1998, doi: 10.1049/ip-gtd:19982182.

[38] S. Pan, “PID controller design of an AVR system,” *Manipal Journal of Science and Technology*, vol. 9, no. 1, 2024, [Online]. Available: https://impressions.manipal.edu/mjst/vol9/iss1/1/

[39] IEEE Standards Association, “IEEE recommended practice for excitation system models for power system stability studies,” *IEEE Std 421.5-2016 (Revision of IEEE Std 421.5-2005)*, pp. 1–207, 2016, doi: 10.1109/IEEESTD.2016.7553421.

## BIOGRAPHIES OF AUTHORS

**Khaled Miloudi** was born in El Oued, Algeria in 1988. He received his B.Sc. degree in electromechanical engineering from Boumerdes University, Algeria, in 2011. His M.Sc. degree was obtained from the Military Polytechnic School in 2017. In 2024, he received his Ph.D. degree in Electrical Engineering from Houari Boumediene University of Science and Technology, Bab-Ezzouar, Algeria. His areas of interest are electrical drives and process control, renewable energy, and the application of artificial intelligence techniques. He can be contacted at email: miloudi-khaled@univ-eloued.dz or khaled.miloudi.dz@gmail.com.

**Ali Medjghou** received the bachelor's degree in Automatic, master's degree in advanced automatic from the Electrical Engineering Department, University of Biskra, Algeria, and doctorate degree in robotics and artificial intelligence from Electronics Department, University of Batna 2, Algeria. He is a member of the research team at (LAAAS) laboratory, University of Batna 2. Currently, he is a lecturer at Tipaza University Center, Algeria. His research interests include artificial intelligence, robotics, automation, soft computing, and control of renewable energy sources for energy management. He can be contacted at email: medjghou.ali@cu-tipaza.dz or a.medjghou@univ-batna2.dz.

**Ala Eddine Djokhrab** was born in El Oued, Algeria in 1982. He received the B.Sc. in 2000. He received a state engineer degree in automatic from Biskra University, Algeria, in 2006. His M.Sc. degree was obtained from Biskra University, Algeria, in 2015. His areas of interest are trajectory tracking for mechanical systems subject to unilateral constraints, control and diagnosis of energy conversion systems, control strategies for humanoid robots, robot control and tracking, development of the audiovisual capabilities of the humanoid robot, contribution to the control of non-regular mechanical systems, and application of artificial intelligence techniques. He can be contacted at email: ali-djokhrab@univ-eloued.dz or aliatun@gmail.com.

**Mosbah Laouamer** was born in El Oued, Algeria, in 1987. He received his master's degree in electrical engineering in 2012 from El-Oued University, Algeria. In 2019, he obtained his doctorate in electrical networks from Yahia Fares University, Medea, Algeria. His areas of interest include phasor measurement units, electrical networks and optimization, power factor improvement, diagnosis and monitoring faults in solar panels, control systems, renewable energy, and the application of artificial intelligence techniques. Currently, he serves as a lecturer and researcher, class B at El-Oued University. He can be contacted at email: laouamer-mosbah@univ-eloued.dz.

**Souhaib Remha** was born in El Oued, Algeria, in 1989. He obtained his master's degree from the Department of Electrical Engineering, El Oued University in 2013. In 2022, he earned his Ph.D degree in Electrical Power Systems from Amar Telidji University, Laghouat, Algeria. Currently, he is a lecturer and researcher at El Oued University, Algeria. His areas of research include planning and optimization problems in electrical power systems, reactive power static compensator, optimization techniques, and artificial intelligence. He can be contacted at email: remha-souhaib@univ-eloued.dz.

**Yacine Aoun** is a Professor at University of El-Oued, Algeria. holds DEUA, B.Sc., M.Sc., and Doctorat Es-Science grades in Mechanical Engineering from Biskra University, Algeria, in 1999, 2002, 2005, 2009, and 2016, respectively. Currently, he is lecturing in the Department of Mechanical Engineering, Faculty of Technology, University of El-Oued, Algeria. He completed his Habilitation in Mechanical Engineering in 2019 at the University of Biskra, Algeria. His research interest includes energy and renewable energy, as well as thin films. He can be contacted at email: aoun28071979@yahoo.fr or aoun-yacine@univ-eloued.dz.